

Lehman, J. and Lakes, R. S., "Stiff lattices with zero thermal expansion", adapted from
Journal of Intelligent Material Systems and Structures, **23** (11) 1263-1268 July (2012)

Stiff lattices with zero thermal expansion

Jeremy Lehman and Roderic Lakes *

Department of Engineering Physics
 Engineering Mechanics Program;
 Materials Science Department and Rheology Research Center
 University of Wisconsin-Madison
 1500 Engineering Drive, Madison, WI 53706-1687
 * address correspondence to RL: e-mail- lakes@engr.wisc.edu

Abstract

Lattice microstructures are presented with zero coefficient of thermal expansion. These are made of positive expansion materials. The behavior is primarily stretch dominated, resulting in favorable stiffness. Behavior of these lattices is compared with that of triangular and hexagonal honeycombs in a modulus-density map. These lattices do not undergo thermal buckling, in contrast to designs based on sub-lattices.

Introduction

Thermal expansion¹ of materials is pertinent in the context of materials that in service may experience temperatures which vary considerably. Materials of zero or minimal thermal expansion can enable designs of structures that are dimensionally stable as temperature varies. By contrast, extremely large expansion is of interest in the context of composite theory and in applications in actuators controlled by temperature changes. In homogeneous crystalline materials thermal expansion is attributed to slight nonlinearity (anharmonicity) of the interatomic potential. It has been therefore considered to be a property intrinsic to each material and not subject to control.

Composite materials had been thought to be limited in their expansion by the expansion coefficients of the constituent phases. Specifically the bounds for the thermal expansion coefficient α of isotropic composite materials² of two solid phases in terms of constituent coefficients of thermal expansion α_1 and α_2 , bulk moduli K_1 and K_2 , are as follows

$$\alpha = \alpha_1 V_1 + \alpha_2 (1 - V_1), \quad (1)$$

$$\alpha = \alpha_1 V_1 K_1 / K + \alpha_2 (1 - V_1) K_2 / K, \quad (2)$$

in which V_1 is the volume fraction of phase 1 and K is the bulk modulus of the composite. The composite expansion can clearly be no higher or lower than that of either of the constituents. Such analysis suggests extremely high expansion is not possible and that zero expansion composites require a constituent of negative expansion. Negative expansion materials such as zirconium tungstate, are known though they are not typical structural materials^{3 4 5}. Bounds on thermal expansion as with bounds on elastic modulus of composites^{6 7 8} depend on assumptions that the two phases are perfectly bonded, that there is no porosity, and that each phase has a positive definite strain energy. Bounds can be useful to predict possible ranges of properties of composites or biological tissues in which the structure is so complicated that one cannot easily analyze the relation between structure and physical properties. However, if one relaxes any of the assumptions, it becomes possible to exceed the bounds. Specifically one can attain expansion values higher than the upper bound or lower than the lower bound.

For example by allowing porosity (void space), with two solid phases of different expansion, one can achieve arbitrarily high positive or negative thermal expansions⁹ in lattices or honeycombs. The lattices and honeycombs contain rib elements each of which is a bi-layer made of two bonded

layers of differing thermal expansion coefficient. Such lattices are in contrast to honeycomb or foam with homogeneous ribs for which the thermal expansion¹⁰ is the same as that of the solid from which it is made. When provided with this concept, it is then possible to design high expansion composites with the aid of topology optimization¹¹. The amount of void space can tend to zero, giving rise to dense composites with slip interfaces. These also can exhibit extreme values of expansion¹². Three-phase bounds (which also assume positive definite strain energy)^{13 14} may be then be applied to lattices when provided with the notion of importance of void space. Large regions of the expansion - modulus map are made accessible via two and three dimensional cellular solids with bi-material rib elements. Positive or negative expansion values of arbitrarily large magnitude or zero are possible¹⁵. Expansion tends to zero as the rib curve angle becomes small.

Zero expansion materials and structures are at times designed to be stiff. In that vein it is expedient to distinguish structures that are bend dominated from those that are stretch dominated. Hexagonal honeycombs (two dimensional lattices) with initially straight ribs of material with modulus E_s of thickness t and length l governed by rib bending and have elastic modulus E as follows¹⁰:

$$E/E_s = 2.3 (t/l)^3. \quad (3)$$

Triangular cell lattices^{10, 16} are stretch dominated and are therefore stiffer.

$$E/E_s = (\sqrt{3}/2) (t/l). \quad (4)$$

Ribs in triangular lattices were assumed to be attached by pin joints to simplify the analysis to include only axial force. By contrast a hexagonal lattice with pin joints has zero structural rigidity therefore the ribs must be solidly joined. The lattices and foams designed to achieve extremely high or negative expansion have highly curved ribs and are bend dominated, hence relatively compliant. Here we present triangular lattices with ribs with minimal curvature, to attain higher stiffness.

Lattice design

The lattice entails a 2D honeycomb lattice designed to obtain a zero thermal expansion while simultaneously maximizing the material's mechanical stiffness and providing immunity from thermal buckling. The lattice thermal expansion coefficient (CTE) is determined as a function of geometrical and material parameters and the result is used to design zero expansion lattices. Moreover the overall mechanical stiffness is determined. Additionally, interpretation of analytical results is provided with the intent of gaining useful design insight.

The honeycomb lattice structure analyzed is shown in **Figure 1**. It is composed of curved bi-material rib elements. The two materials have differing thermal expansion coefficients which subject the rib element to deformation attributed to bending as well as axial deformation. This allows, through the careful tuning of geometric and material property parameters, an overall thermal expansion coefficient of zero. A triangular cell was chosen to maximize stiffness, since at small curvatures the mechanical stiffness is dominated by axial deformations. The following sections will explain how the thermal expansion coefficient and mechanical stiffness are determined analytically.

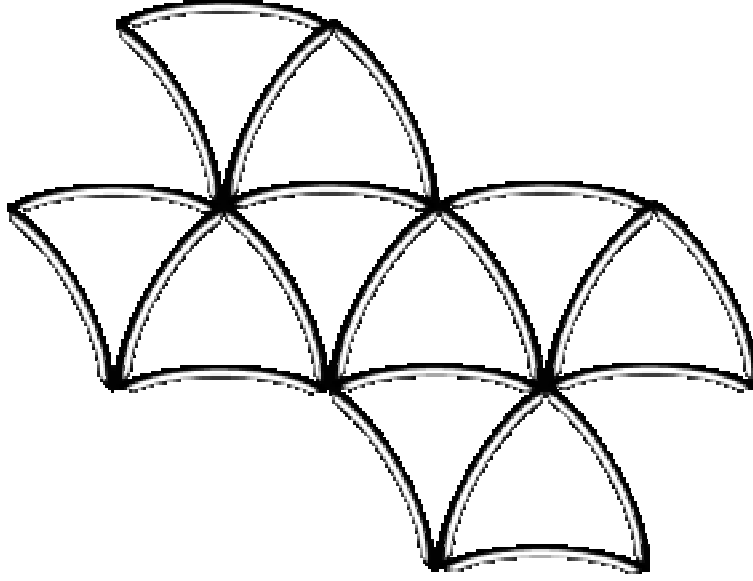


Figure 1 showing a lattice structure composed of equilateral triangular cells made of curved bi-material rib elements. Material one, with a smaller thermal expansion coefficient, is shown in white while the higher coefficient of expansion material two, is shown in black.

Results

Thermal expansion coefficient α

The thermal expansion coefficient α (CTE) of the lattice is calculated from the axial displacement of each rib element in the lattice due to temperature change. The analysis, as with the high expansion lattices, is based on that of Timoshenko¹⁷ for bi-material curved bars. Assumptions made include the usual elementary bending assumptions of a slender bar subject to small deflection, properties that remain constant in time, an ideal slip free joint between materials in each rib, plane sections remain plane. Moreover in the context of the lattice, rib elements are assumed to be connected by pin joints so they transmit only a force, and that the ribs do not contact each other; also that the curve angle is small. In prior study¹⁵ of lattices of extreme expansion, some simplifying assumptions were used to aid design and visualization. Specifically, it was assumed that the circumferential extension of the element is negligible compared to the change in geometry caused by bending, also, that the rib element is composed of materials having equal thicknesses and Young's moduli.

$$\alpha_{Bend} = (\alpha_2 - \alpha_1) \frac{L_{arc}}{t} \left[\frac{1}{2} \cot\left(\frac{\theta}{2}\right) - \frac{1}{\theta} \right] \quad [\text{Eq. 1}]$$

in which α_1 and α_2 are the component materials' thermal expansion coefficients, t is the total thickness of the rib, L_{arc} is the length of the rib element and θ is the included angle. If the angle is not too large, this expression assumes a simpler form, with $t = h_1 + h_2$, $\alpha = (l/t) (\alpha_1 - \alpha_2) (\theta / 12)$.

For the small curvatures required to attain zero expansion the axial extension can no longer be neglected. In the present analysis the general form given by Timoshenko is applied to bi-material bars with small curvature in which stretch, shear and bend all contribute to the deformation. A generalized form which allows for differing material thicknesses as well as Young's moduli was obtained⁹ from the bi-material bar relations¹⁷.

$$\alpha_{Bend} = (\alpha_2 - \alpha_1) \frac{L_{arc}}{t} \left[\frac{1}{2} \cot\left(\frac{\theta}{2}\right) - \frac{1}{\theta} \right] \frac{6(1+m)^2}{3(1+m)^2 + (1+mn)\left(m^2 + \frac{1}{mn}\right)} \quad [\text{Eq. 2}]$$

For sufficiently small angles Equation 2 reduces to the following.

$$\alpha_{Bend} = (\alpha_1 - \alpha_2) \frac{L_{arc}}{t} \left(\frac{\theta}{12}\right) \frac{6(1+m)^2}{3(1+m)^2 + (1+mn)\left(m^2 + \frac{1}{mn}\right)} \quad [\text{Eq. 3}]$$

The variable m is the ratio of material one's thickness to material two's thickness and n is the ratio of material one's Young's modulus to material two's Young's Modulus.

The longitudinal expansion term is derived from the longitudinal strain at the material interface described by Timoshenko¹⁷. The axial thermal expansion term is obtained by dividing by the change in temperature and by assuming sufficiently small angles (so that $\sin \theta \approx \theta$) as in Equation 4.

$$\alpha_{Axial} = \frac{\alpha_1 + \alpha_2}{2} + (\alpha_2 - \alpha_1) \left[\frac{4m^2 + 3m + \frac{1}{nm}}{nm^3 + 4m^2 + 6m + \frac{1}{nm} + 4} - \frac{1}{2} \right] \quad [\text{Eq. 4}]$$

The axial term is added directly to the previous result for thermal expansion due to rib bending to obtain the total overall CTE of the rib element. This CTE is also the macroscopic value for the lattice structure depicted in **Figure 1**. The total thermal expansion coefficient is given by Equation 5.

$$\alpha = (\alpha_1 - \alpha_2) \frac{L_{arc}}{t} \left(\frac{\theta}{12}\right) \frac{6(1+m)^2}{3(1+m)^2 + (1+mn)\left(m^2 + \frac{1}{mn}\right)} + \frac{\alpha_1 + \alpha_2}{2} + (\alpha_2 - \alpha_1) \left[\frac{4m^2 + 3m + \frac{1}{nm}}{nm^3 + 4m^2 + 6m + \frac{1}{nm} + 4} - \frac{1}{2} \right] \quad [\text{Eq. 5}]$$

From this relationship, it is possible to tune the CTE to be zero by carefully choosing geometric and material properties. The graph shown in **Figure 2** shows the included angle theta necessary to achieve an overall CTE of zero. The rib aspect ratio, AR , is the ratio the rib arc length to the rib thickness. Each of the curves represents a different aspect ratio for comparison. Material one was considered to be Invar, while steel was used as material two. The thermal expansion coefficient values for materials one and two were 1 and 12 ($\mu\text{strain}/\text{K}$) respectively¹⁸ (ASM International, 2002). For this plot typical modulus values of 140 GPa¹⁹ for Invar and 200 GPa for steel were used. The plot was obtained by numerically varying the invar fraction, which is the percentage of total rib material that is invar, from zero to one hundred and then solving for the required angle θ in order to achieve a zero thermal expansion.

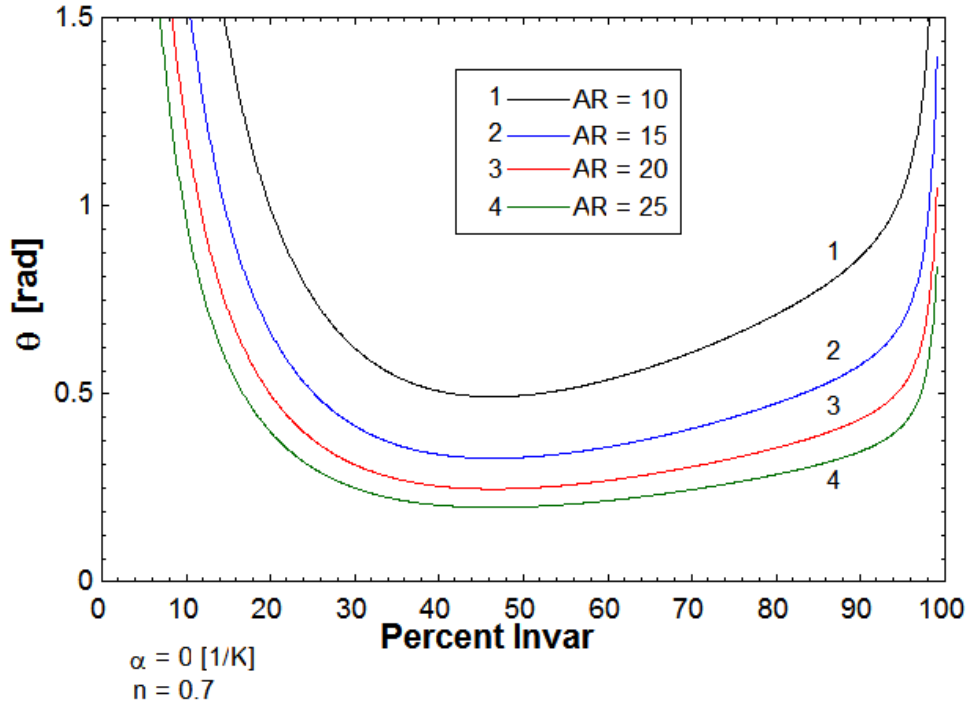


Figure 2 shows the required curvature in terms of included angle versus the proportion of Invar, for various rib aspect ratios.

In order to maximize stiffness it is desirable to have a smaller included angle which corresponds to a less curved rib element. An optimum value for invar fraction is observed at approximately 45 percent. The angle can also be reduced by specifying the rib element to be more slender. Slender ribs entail a more compliant lattice.

Equation 5 determines the theoretical thermal expansion for a triangular honeycomb made of curved bi-material rib elements. This equation allows for the thermal expansion to be optimized to zero. In order to optimize the material stiffness a similar equation for the total material stiffness is required.

Lattice elastic modulus

The equation for overall mechanical stiffness Young's modulus E_H of the lattice is obtained by first finding the relationship for the deformation in terms of an applied load P . This analysis relies on the assumption that the rib elements are pin connected at the lattice nodes. **Figure 3** shows the loading state on a single rib element.

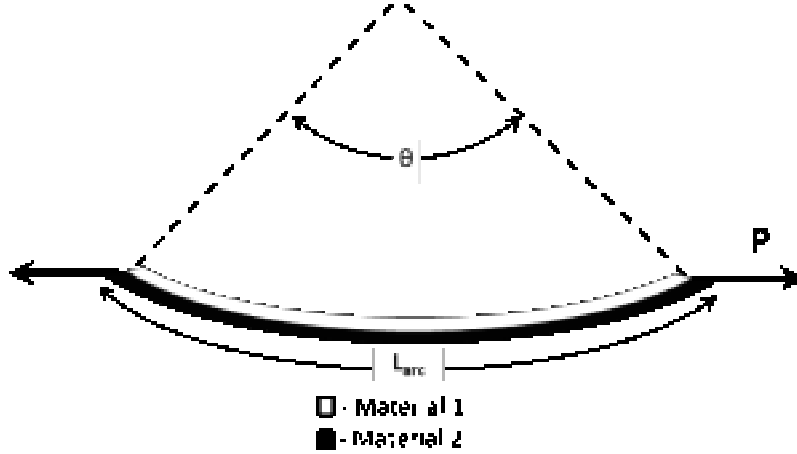


Figure 3 showing the loading used for determining the deformation of a single element.

The horizontal deformation of the rib element can be found by applying standard formulae²⁰ for circular arches. Application of these formulae results in three deflection terms. The first term is a result of bending, the second a result of axial deformation and the third term is a result of shear deformation. They are given below as Equations 6-8, where G is the effective shear modulus of the entire rib element.

$$\delta_{\text{Bend}} = P \left(\frac{L_{\text{arc}}}{t} \right)^3 \frac{12(m+1)}{E_1 m + E_2} \left[\frac{\cos^2\left(\frac{\theta}{2}\right) + \frac{1}{2}}{\theta^2} - \frac{3 \sin\left(\frac{\theta}{2}\right) \cos\left(\frac{\theta}{2}\right)}{\theta^3} \right] \quad [\text{Eq. 6}]$$

$$\delta_{\text{Axial}} = -P \left(\frac{L_{\text{arc}}}{t} \right) \frac{m+1}{E_1 m + E_2} \left[\frac{1}{2} - \frac{3 \sin\left(\frac{\theta}{2}\right) \cos\left(\frac{\theta}{2}\right)}{\theta} \right] \quad [\text{Eq. 7}]$$

$$\delta_{\text{Shear}} = P \left(\frac{L_{\text{arc}}}{t} \right) \frac{6}{5G} \left[\frac{1}{2} - \frac{\sin\left(\frac{\theta}{2}\right) \cos\left(\frac{\theta}{2}\right)}{\theta} \right] \quad [\text{Eq. 8}]$$

To obtain the total deformation these three terms are summed. Structural spring compliance (J_{str}) is expressed as the deformation normalized by load P . Plots showing all three structural spring compliances versus the included angle are given in **Figure 4** and **Figure 5**. The Invar fraction was set to 45 percent and rib aspect ratio to 10 and 25. Typical modulus values of 140 GPa²¹ and 200 GPa were used for the stiffness values of Invar and steel respectively.

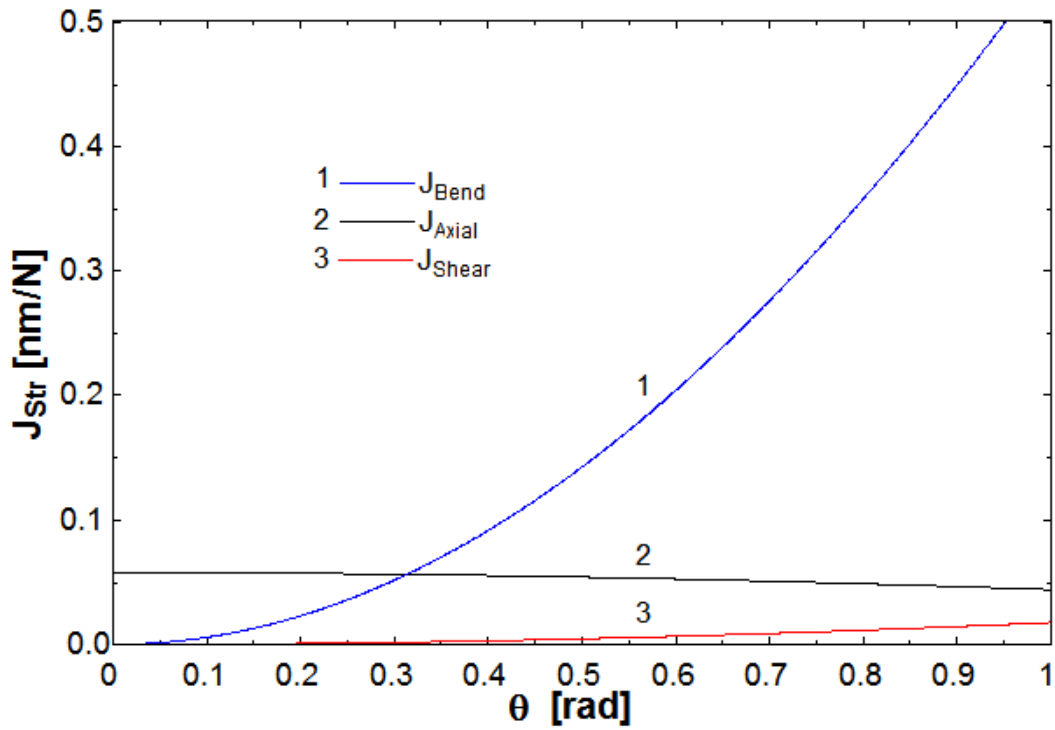


Figure 4 shows a comparison of the three terms contributing to horizontal structural spring compliance versus the included angle for a rib aspect ratio of 10.

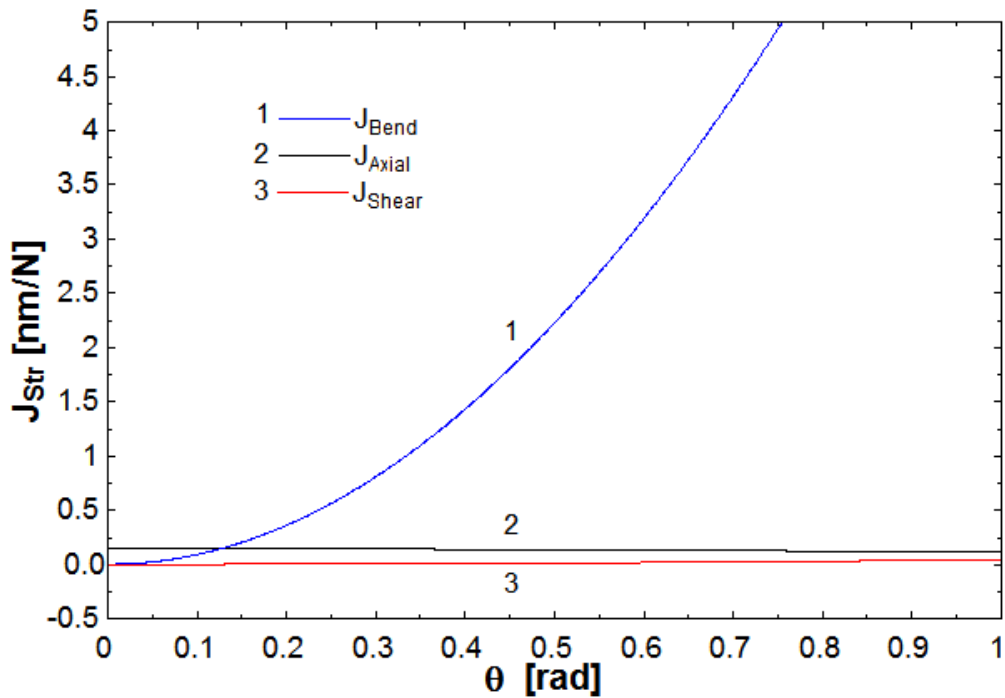


Figure 5 shows a comparison of the three terms contributing to horizontal structural spring compliance versus the included angle for a rib aspect ratio of 25.

Figure 4 indicates that it is possible to obtain a rib in which the largest term in the compliance is axial deformation rather than bending for relatively large included angles. It also can be seen that the shear deformation term can be neglected for the range of included angles that are practical. **Figure 5** demonstrates that more slender the rib elements become bending dominated at smaller curve angles. The effect of shear deformation is negligible for both rib aspect ratios and is neglected in the sum of deformations. Equation 9 provides the total horizontal deformation for a given load P.

$$\delta_{\text{sum}} = P \left(\frac{L_{\text{arc}}}{t} \right)^3 \frac{12(m+1)}{E_{1m} + E_2} \left[\frac{\cos^2\left(\frac{\theta}{2}\right) + \frac{1}{2}}{\theta^2} - \frac{3 \sin\left(\frac{\theta}{2}\right) \cos\left(\frac{\theta}{2}\right)}{\theta^3} \right] - P \left(\frac{L_{\text{arc}}}{t} \right) \frac{m+1}{E_{1m} + E_2} \left[\frac{1}{2} - \frac{3 \sin\left(\frac{\theta}{2}\right) \cos\left(\frac{\theta}{2}\right)}{\theta} \right] \quad [\text{Eq. 9}]$$

Once the horizontal deflection is solved for the overall mechanical stiffness for the triangular honeycomb can be obtained by applying the same technique used by Hunt ¹⁶. The ribs are approximated as pin connected and thus act as two-force members. This method results in identical equilibrium equations as those derived by Hunt. This derivation accounts for the differing geometry and the additional bending deflection term. The total mechanical stiffness of the honeycomb lattice depicted in **Figure 1** is given by Equation 10.

$$E_h = \frac{2}{\sqrt{3}} \left(\frac{t}{L_{\text{arc}}} \right) \frac{E_{1m} + E_2}{m+1} \left[\frac{2 \theta^3}{24 \left(\frac{L_{\text{arc}}}{t} \right)^2 \left(\frac{\theta}{2} \cos(\theta) + \theta - \frac{3}{2} \sin(\theta) \right) + 3 \theta^2 \sin(\theta) - \theta^3} \right] \quad [\text{Eq. 10}]$$

It is worth noting that as the included angle approaches zero an identical equation to that of Hunt's is obtained. The parameters of Equation 10 were varied numerically. The plot in **Figure 6** shows the total stiffness of the honeycomb structure versus Invar fraction. Each curve represents a different rib aspect ratio, and is constrained to have an overall thermal expansion coefficient of zero. Material properties used are typical for Invar and steel.

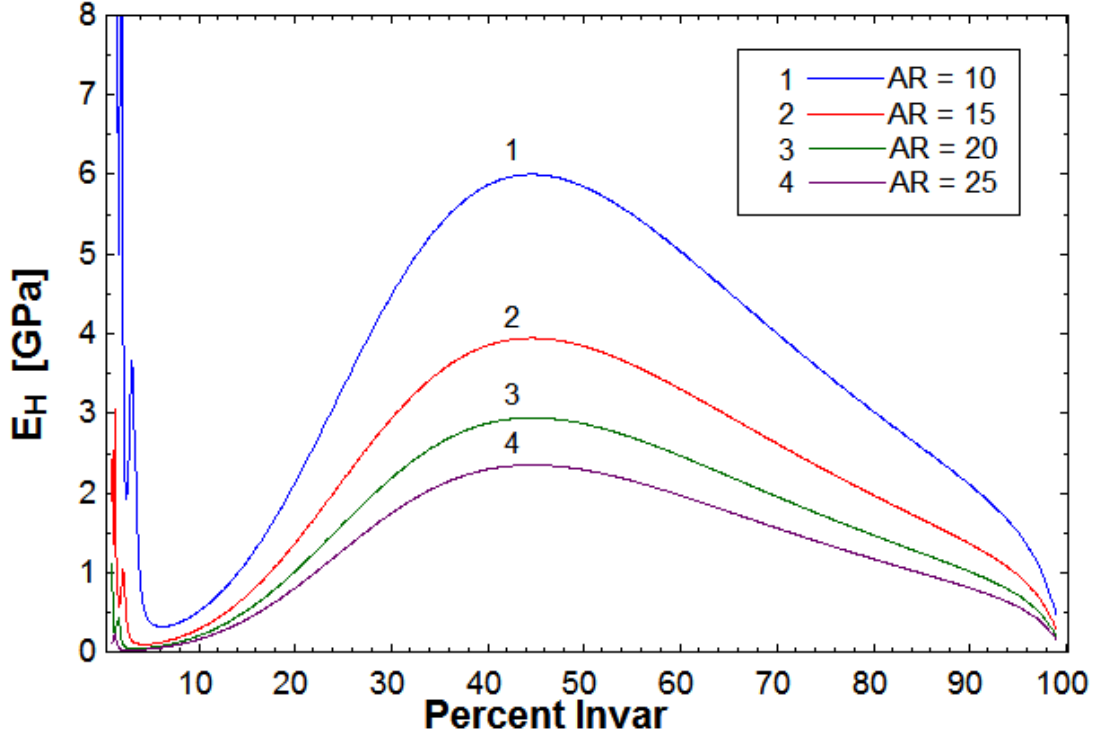


Figure 6 shows total mechanical stiffness versus the Invar fraction for various rib aspect ratios. Thermal expansion is constrained to be zero.

An optimal Invar fraction exists of approximately 45%. It can also be seen that by reducing the slenderness of the rib elements the overall stiffness is increased. Reducing the slenderness too far, however, invalidates the assumption of slender beams leading to a larger discrepancy between the predicted and actual values of thermal expansion and stiffness.

Figure 7 shows normalized elastic modulus vs. rib thickness ratio (t/L_{arc}) for zero expansion steel-invar triangular lattices with curved ribs, compared with theoretical plots for triangular and regular hexagonal lattices with straight ribs. The theoretical lines after Gibson and Ashby¹⁰ show that an axially dominated lattice structure has relative stiffness following a curve proportional to the ratio t/L whereas a bending dominant structure's relative stiffness¹⁰ is proportional to the ratio $(t/L)^3$. The specific equations relating relative stiffness for equilateral triangle and regular hexagon lattices are given by Equations 11 and 12 respectively, from Gibson and Ashby¹⁰.

$$\frac{E_H}{E_S} = 1.15 \left(\frac{t}{L_{arc}} \right) \quad [\text{Eq. 11}]$$

$$\frac{E_H}{E_S} = 2.3 \left(\frac{t}{L} \right)^3 \quad [\text{Eq. 12}]$$

The zero expansion lattice follows the same slope as the equilateral triangular lattice but a factor of 3.4 lower in modulus. By contrast the bend dominated hexagonal lattice is a factor of 92 more compliant than the stretch (axial) dominated triangular zero expansion lattice for $L/t = 25$; the factor increases with slenderness. Therefore the present zero expansion lattice is axial dominated with a modest stiffness reduction due to a superposed bending of the curved ribs.

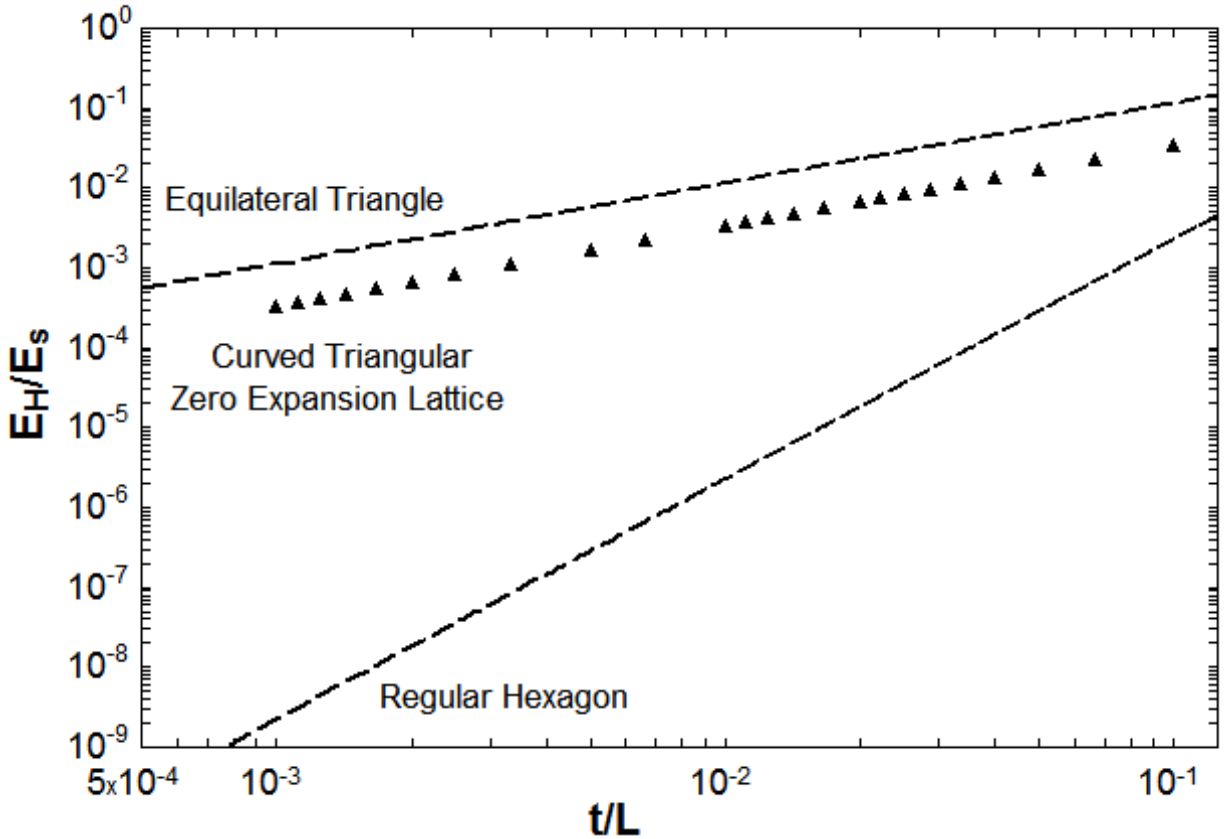


Figure 7 compares analytically determined stiffness ratios for optimally designed curved rib zero expansion lattices with elements composed of Steel and Invar with straight rib triangular lattices that are fully axial dominated and hexagonal lattices that are fully bending dominated.

Discussion

The lattices presented here contain bi-material ribs. It is also possible to make lattices of low or zero expansion using several kinds of ribs each of which is homogeneous²². Such lattices will provide zero expansion and high, near optimal stiffness if the temperature range is not too great but they will buckle under sufficient temperature because each kind of rib has a different expansion coefficient. For example, the critical buckling load of a pin end column of circular section of diameter d and length L , Young's modulus E and section moment of inertia I is $P_{cr} = \pi^2 EI/L^2$ with $I = \pi d^4/64$ for a round section. The corresponding buckling strain is $\varepsilon_{cr} = (\pi^2/16) (d/L)^2$. For $d/L = 1/25$, the strain for buckling is 0.001. Ribs made of aluminum alloy with $\alpha = 24$ ppm/ $^\circ\text{C}$, if fully constrained by another lattice, will experience a strain $\varepsilon = \alpha \Delta T$ and will buckle under a temperature difference of only $\Delta T = 42$ $^\circ\text{C}$. If the second lattice has nonzero expansion, it will provide a partial constraint so the allowable temperature range will be greater but not by much. For environments that impose greater temperature excursions, the present lattices offer the advantage of no buckling of ribs under temperature changes at the expense of a moderate reduction in stiffness.

Minimal or zero thermal expansion can also be achieved in two phase composites (without void content) with inclusions of negative expansion or of negative stiffness²³. Composites with negative stiffness inclusions via incipient phase transformations have extremely high damping capacity²⁴; also, extreme Young's modulus²⁵ exceeding that of diamond but thermal expansions have not been measured in these.

Conclusion

Triangular lattices of curved bi-material ribs are designed that provide zero thermal expansion and a stiffness approaching that of a fully axial dominated lattice. The modest penalty in stiffness is compensated by the fact that these lattices are not subject to thermal buckling.

References

- ¹ I. S. Sokolnikoff, *Mathematical theory of elasticity*, (Krieger, Malabar, FL, 2nd ed., 1983).
- ² J. L. Cribb, "Shrinkage and thermal expansion of a two-phase material", *Nature*, **220**, 576-577 (1963).
- ³ C. Martinek and F. Hummel, Linear thermal expansion of three tungstates, *J. Am. Ceramic Soc.* **51**, 227-228, (1968).
- ⁴ T. A. Mary, J. S. O. Evans, T. Vogt and A. W. Sleight, "Negative thermal expansion from 0.3 to 1050 Kelvin in ZrW₂O₈" *Science*, **272**, 90-92, (1996).
- ⁵ J. S. O. Evans, T. A. Mary and A. W. Sleight, "Negative thermal expansion materials", *Physica B*, **241**, 311-316 (1997).
- ⁶ B. Paul, "Prediction of elastic constants of multiphase materials", *Trans. ASME*, **218**, 36, (1960).
- ⁷ Z. Hashin, "Analysis of composite materials- a survey", *J. Applied Mechanics*, **50**, 481-505 (1983).
- ⁸ G. Milton, *The Theory of Composites*, Cambridge University Press, (2002).
- ⁹ R. S. Lakes, "Cellular solid structures with unbounded thermal expansion", *Journal of Materials Science Letters*, **15**, 475-477 (1996).
- ¹⁰ L. J. Gibson and M.F. Ashby, *Cellular Solids*, 2nd edition, Cambridge, UK, (1997).
- ¹¹ O. Sigmund and S. Torquato, Composites with extremal thermal expansion coefficients, *Appl. Phys. Lett.*, **69**, 3203-3205, (1996).
- ¹² R. S. Lakes, "Dense solid microstructures with unbounded thermal expansion", *J. Mechanical Behav. Mts.*, **7**, 85-92, (1996).
- ¹³ R. A. Schapery, "Thermal expansion coefficients of composite materials based on energy principles", *J. Composite Materials*, **2**, 380-404, 1968.
- ¹⁴ Rosen, B. W. and Hashin, Z., Effective thermal expansion and specific heat of composite materials, *Int. J. Engng. Sci.* **8**, 157-173, 1970.
- ¹⁵ R. S., Lakes, "Solids with tunable positive or negative thermal expansion of unbounded magnitude", *Applied Phys. Lett.* **90**, 221905 (2007).
- ¹⁶ H. E. M. Hunt, The mechanical strength of ceramic honeycomb monoliths as determined by simple experiments, *Transactions of the Institution of Chemical Engineers* **71A** 257-266, 1993.
- ¹⁷ S. P. Timoshenko, "Analysis of bi-metal thermostats", *J. Optical Soc. America*, **11**, 233-355 (1925).
- ¹⁸ ASM International. (2002). *ASM ready reference. Thermal properties of metals*. Materials Park, Ohio.
- ¹⁹ C. Woolger, (1996, June). Invar nickel-iron alloy : 100 years on. *Materials World*, **4**, 332-333.
- ²⁰ W. C. Young, (1989). *Roark's Formula's for Stress and Strain* (6th ed.). New York: McGraw-Hill Book company.
- ²¹ C. Woolger, (1996, June). Invar nickel-iron alloy : 100 years on. *Materials World*, **4**, 332-333.
- ²² C. A. Steeves, S. L. dos Santos e Lucato, M. He, E. Antinucci, J. W. Hutchinson, A. G. Evans, Concepts for structurally robust materials that combine low thermal expansion with high stiffness, *Journal of the Mechanics and Physics of Solids*, **55**, 1803-1822, 2007.

²³ Y. C. Wang and R. S. Lakes, "Extreme thermal expansion, piezoelectricity, and other coupled field properties in composites with a negative stiffness phase", *Journal of Applied Physics*, **90**, 6458-6465, Dec. (2001).

²⁴ R. S. Lakes, T. Lee, A. Bersie, and Y. C. Wang, "Extreme damping in composite materials with negative stiffness inclusions", *Nature*, **410**, 565-567, (2001).

²⁵ T. Jaglinski, D. S. Stone, D. Kochmann, and R. S. Lakes, "Materials with viscoelastic stiffness greater than diamond" *Science*, **315**, 620-622, (2007).